Chapter 10
A Galerkin Method Solution of Heat Transfer Problems in Closed Channels: Fluid Flow Analysis

Nasser Ghariban

Introduction

The study of conventional forced convection in channels is a requirement for well-designed heat transfer equipment. A channel is a configuration for studying internal flows. Being well informed or having knowledge of the structure of flow in a channel is of great engineering interest since it can be applied in many applications. Channels contain flows that are considered Newtonian fluid. The traditional application of this study is in heat transfer equipment, such as heat exchangers; the friction factor and heat transfer coefficient are important parameters for evaluating design performance of these equipment. Recently, the growth in microfluidic systems with needs of transporting of liquids or gases in channels with micro cross-sectional dimensions is of great importance in many applications. These applications in microelectronic cooling, MEMS, fuel cell technology, and medical and biomedical devices motivated researchers to investigate on simple solutions for channel flow. Microchannels have specific characteristics such as high surface area per unit volume and high heat transfer coefficient that will provide further application in the future. A study of velocity and temperature distribution in these channels will help investigators to understand the pressure drop and heat transfer rate at the boundaries. Although the behavior of fluid in microchannels is laminar in larger-scale equipment such as heat exchangers, the designer usually deals with turbulent flow. When flow is turbulent, the computations are difficult. Often, the experimental studies of shear stress and heat transfer in turbulent flow guide researchers toward theoretical predictions. However, the experimental data are not universally available for all possible shapes and flow conditions.

N. Ghariban (✉)
Department of Engineering, Virginia State University, Petersburg Virginia 23806, USA
e-mail: nghariban@vsu.edu

B. Toni (ed.), *Advances in Interdisciplinary Mathematical Research*, Springer Proceedings in Mathematics & Statistics 37, DOI 10.1007/978-1-4614-6345-0_10,

Numerical computation has served engineers well and is a powerful tool. This work seeks a simple mathematical model that can produce relatively accurate results with little computational effort. The Galerkin-based method of solution given by Haji-Sheikh et al. [4] and Beck et al. [1] is modified to solve laminar flow in closed channels as well as study of turbulent flow. This method provided a simple and effective method for calculating laminar flow characteristics in various shape channels. It is also shown that this method can also be used for turbulent flow; however, major modifications are needed. A set of basis functions that are markedly different from the basis functions for laminar flow must be selected. Improved accuracy and rapid convergence are realized when the basis functions include the dependence of turbulent viscosity on the velocity gradient. From several different turbulent viscosity models, the Van Driest model is chosen for this solution method. It was determined that a modified Van Driest model provides computed data that agree well with experimental data of other investigators, e.g., Laufer [7] and Nikuradse [9].

Analysis

The objective of this paper is to develop a simple and computationally efficient method for finding flow properties such as pressure drop. The Galerkin method is selected because it is equally applicable to circular and noncircular ducts. The same method has been extended for soling thermal characteristics of the channels that will be address in second part of this publication.

Governing Equations

The Galerkin-based method is a simple technique for finding the velocity field in ducts with arbitrary cross-section areas. For convenience, the Cartesian coordinates are used to describe the method of solution. The cylindrical coordinates are used for study of pipe flow as demonstrated in example 1 and 3 of this study. The momentum equations for fully developed channel flow are

$$\rho \frac{Du}{Dt} = \rho . f - \nabla P + \mu \nabla^2 u \tag{1}$$

In the absence of external forces and steady-state condition, the equation for a laminar flow will simplify to

$$-\frac{\partial P}{\partial Z} + \mu \left(\frac{\partial^2 w}{\partial x^2} + \frac{\partial^2 w}{\partial y^2} \right) = 0 \tag{2a}$$

where w is the velocity of the flow along channel axis (z).

For turbulent flow the equation will have an extra term due to fluctuation of velocity along x, y, and z axis as

$$-\frac{\partial P}{\partial z}+\mu\left(\frac{\partial^2 w}{\partial x^2}+\frac{\partial^2 w}{\partial y^2}\right)-\rho\left(\frac{\overline{\partial u'w'}}{\partial x}+\frac{\overline{\partial v'w'}}{\partial y}\right)=0 \tag{2b}$$

The Boussinesq's eddy-diffusivity coefficients for momentum are defined as

$$\begin{aligned} -\rho\overline{u'w'} &= \mu_t \tfrac{\partial w}{\partial x} \\ -\rho\overline{v'w'} &= \mu_t \tfrac{\partial w}{\partial y} \end{aligned} \tag{3}$$

The following equation is given by substituting the above expressions into Eq. (2b)

$$-\frac{\partial P}{\partial z}+\frac{\partial}{\partial x}\left(\mu_e\frac{\partial w}{\partial x}\right)+\frac{\partial}{\partial y}\left(\mu_e\frac{\partial w}{\partial y}\right)=0 \tag{4}$$

where μ_e is the effective viscosity given as

$$\mu_e=\mu+\mu_t$$

If the vector notation is used, the turbulent momentum equation is shortened to

$$-\frac{\partial P}{\partial z}+\nabla\cdot(\mu_e\nabla w)=0 \tag{5}$$

This equation can be written in nondimensional form as

$$1+\nabla_1\cdot(\mu_e^*\nabla_1 W)=0 \tag{6}$$

where $\mu_e^*=1+(\mu_t/\mu)=1+\mu_t^*$ for laminar flow in absence of eddy-diffusivity $\mu_e^*=1$ and Eq. (6) will be simplified to $1+\nabla_1^2 W=0$

$$W=\frac{\mu w}{-a^2\frac{\partial P}{\partial z}} \text{ where } a \text{ is a characteristic length}$$

and

$$\nabla_1=\frac{\partial}{\partial X}i+\frac{\partial}{\partial Y}j \text{ where } X=x/a \text{ and } Y=y/a$$

Turbulent Viscosity

Equation (6) indicates that the momentum equations contain turbulent viscosity that is a function of the surface sheer stress. Because of the appearance of this term, the mean flow equations are not complete; a turbulent model is necessary to determine the turbulent diffusivity terms before the equations can be solved.

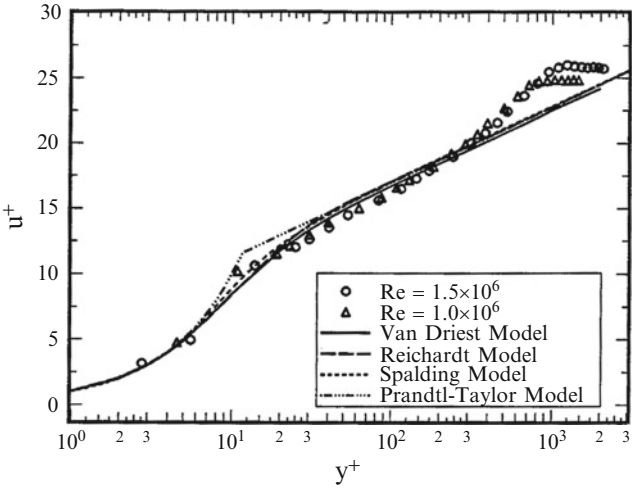

Fig. 10.1 Nondimensional velocity profile for turbulent boundary layer

Kakac et al. [5] has summarized different models of turbulent viscosity for predicting velocity profile inside the turbulent boundary layer. Figure 10.1 shows the velocity distribution from the wall with the nondimensional parameters u^+ and y^+,

$$u^+ = \frac{\overline{u}}{\sqrt{\tau_w/\rho}},\ y^+ = \frac{y\sqrt{\tau_w/\rho}}{\nu}$$

where τ_w is the wall shear stress.

The circular and the triangular symbols are the results of an experimental study for Reynolds number of 1.5×10^6 and 1.0×10^6, respectively, conducted by the author. As Fig. 10.1 illustrates, the Van Driest model is smooth and continuous in the near wall region and follows experimental data with a good agreement. The good prediction of turbulence near the wall by the Van Driest model is the primary reason for its selection. This model is solely a function of y^+; therefore, it would considerably simplify the numerical calculations and increase the accuracy of the results. According to the Van Driest [11] model, the effective viscosity is given as

$$\mu_e = \mu \frac{1 + \{1 + 4\kappa^2 (y^+)^2 [1 - \exp(-y^+/A^+)]^2\}^{1/2}}{2} \tag{7}$$

Researchers who have used the Van Driest model to study turbulent flow inside ducts report that an additional modification is necessary to remove certain inaccuracies. Malhotra and Kang [8] used Eq.(7) with an additional correction factor which

emerged as a result of studies on a two-equation model of turbulence for pipe flow. The turbulence viscosity then becomes

$$\mu_t = \rho\kappa^2 y^2[1-\exp(y^+/A^+)]\left|\frac{\partial u}{\partial y}\right|/(1+\frac{3y}{R}+\frac{3y^2}{R^2})$$

where R is the radius of the pipe and y is the distance from the wall. Richman and Azad [10] assumed a constant turbulence viscosity in the range $0.158 \le y/R \le 1$ as

$$\mu_t = \mu\frac{\{1+4\kappa^2(y^+)^2[1-\exp(-y^+/A^+)]^2\}^{1/2}-1}{2} \tag{8}$$

for $0 \le y/R \le 0.158$ and $\mu_t = (\mu_t)_{y/R=0.158}$ for $0.158 \le y/R \le 1$

In the present study, the second modification yields a closer agreement with the experimental data.

Calculation of Fluid Flow Properties and Pressure Drop

A Galerkin-based integral (GBI) method [1] is used to solve momentum and energy equations. This is based on weighted residual methods. The method can be used for any ordinary differential equation such as $L[y(x)]+f(x)=0$ over interval $a \le x \le b$ where L denotes a linear differential equation.

Multiplying this equation with any arbitrary function w(x) and integrating over the interval [a,b] provide

$$\int_a^b w(x)\{L[y(x)]+f(x)\}dx = 0$$

Weighted residual method provides solution to this equation by introducing a trial solution of u(x) as

$$u(x) = \phi_0(x) + \sum_{j=1}^{n} c_j\phi_j(x)$$

Replacing y(x) with u(x) on the left side of original differential equation, the residual is defined as follows:

$$r(x) = L[u(x)]+f(x)$$

The goal of this method is to construct u(x) so that the integral of the residual will be zero for some choices of weighted functions. This means the following condition, zero residual, must be satisfied for some choices of w(x):

$$\int_a^b w(x)\{L[u(x)]+f(x)\}dx = 0$$

Galerkin Method

Galerkin method is one of the most commonly used weighted residual methods. This method chooses the weight function, w(x), as a function of basis functions, $w(x) \in \phi_i(x)|_{i=1}^{n}$

$$\int_a^b \phi_i(x)\{L[u(x)] + f(x)\}dx = 0 \qquad \text{for} \quad i = 1,2,\ldots\ldots,n$$

Introducing trial function, $u(x) = \phi_0(x) + \sum_{j=1}^{n} c_j\phi_j(x)$, into this equation provides a set of n equations that must be solved to find the coefficients of basis functions C_j:

$$\int_a^b \phi_i(x)\left\{L\left[\sum_{j=1}^{n} c_j\phi_j(x)\right] + L[\phi_o(x)] + f(x)\right\}dx = 0 \quad \text{for} \quad i = 1,2,\ldots\ldots,n \quad (9)$$

Solution of the Momentum Equation

Equation (6) is the momentum equation in nondimensional space with the boundary condition $V = 0$ on the wall. According to the Galerkin-based integral method, the solution is approximated as a linear combination of a set of basis functions

$$V(X,Y) = \sum_{i=1}^{N} c_i f_i(X,Y) \tag{10}$$

The basis functions, f_i, are linearly independent and satisfy the same homogeneous boundary conditions as V; thus, $V(X,Y)$, axial velocity in Z direction, satisfies the given boundary conditions for all choices of the c_i's. Next, if the error or residual is formed and the d_i's are chosen so that the weighted integral of the residual is zero for each $i = 1,\ldots,N$, a linear algebraic system is obtained as

$$\mathbf{A}\cdot\mathbf{c} = \mathbf{b} \tag{11}$$

where **d** is the vector of coefficients which has the elements $d_1, d_2, \ldots, d_N$ and it is the solution of the above system of N linear equations. The vector **g** has elements

$$b_i = -\frac{1}{A}\int_A f_i dA \tag{12}$$

and the matrix **A** has the elements

$$a_{ij} = \frac{1}{A}\int_A f_i \nabla_1 \cdot (\mu_e^* \nabla_1 f_j) \quad \text{for turbulent flow} \tag{13a}$$

$$a_{ij} = \frac{1}{A}\int_A f_i \nabla_1 \cdot (\nabla_1 f_j) \quad \text{for laminar flow} \tag{13b}$$

The solution of Eq. (11) results in the evaluation of coefficients, $c_1, c_2, \ldots, c_N$, and their substitution in Eq. (10) yields the solution for velocity V.

Haji-Sheikh et al. [4] derived the following equations for skin friction and dimensionless velocity by this method:

$$C_f \mathrm{Re} = \frac{2D_e^2}{a^2 V_{av}} = \frac{2\overline{D_e^2}}{V_{av}} \tag{14}$$

$$\frac{V}{V_{av}} = \frac{V}{V_{av}} = \frac{C_f \mathrm{Re}}{2\overline{De^2}} \sum_{i=1}^{N} d_i f_i \tag{15}$$

where $C_f = -(\partial_P/\partial_Z)D_e/(\rho v_{av}/2) = 4\tau_w/(\rho v_{av}/2)$, $\mathrm{Re} = \rho D_e v_{av}/\mu$, and D_e/a is designated as the nondimensional hydraulic diameter.

The solution for laminar flow has simple steps of defining suitable basis functions, solving array $\boldsymbol{b}$ and matrix $\boldsymbol{a}$ Eqs. (12) and (13b), and then solving for array $\boldsymbol{c}$ to find velocity profile from Eq. (10).

The momentum equation for turbulent flow to solve is more complex. The turbulent viscosity (μ_e^*) is a function of wall shear stress (τ_w) that must be determined. An iterative method is used to solve this equation for turbulent flow. Figure 10.2 demonstrates the flow chart for this solution.

Example 1: Laminar Pipe Flow

The momentum equation in cylindrical coordinate can be written as $-\frac{dP}{dz} + \mu\left[\frac{1}{r}\frac{d}{dr}\left(r\frac{dv}{dr}\right)\right] = 0$ with boundary condition of $v = 0$ at $r = R_0$. (R_0 is the radius of the pipe.)

Introducing nondimensional velocity as

$$V = -\frac{\mu v}{R_o^2(dP/dz)} \quad \text{and} \quad R = \frac{r}{R_o}$$

the equation reduces to

$$\left[\frac{1}{R}\frac{d}{dr}\left(R\frac{dV}{dR}\right)\right] + 1 = 0 \text{ with boundary condition of } V = 0 \text{ at } R = 1$$

The exact solution for this equation is

$$V = \frac{1}{4}(1 - R^2)$$

Dividing it by average velocity, it can be normalized to $U^* = \frac{V}{V_{ave}} = 2(1 - R^2)$

And the exact solution for skin friction using Eq. (9) can be evaluated as $C_f \mathrm{Re} = 64$.

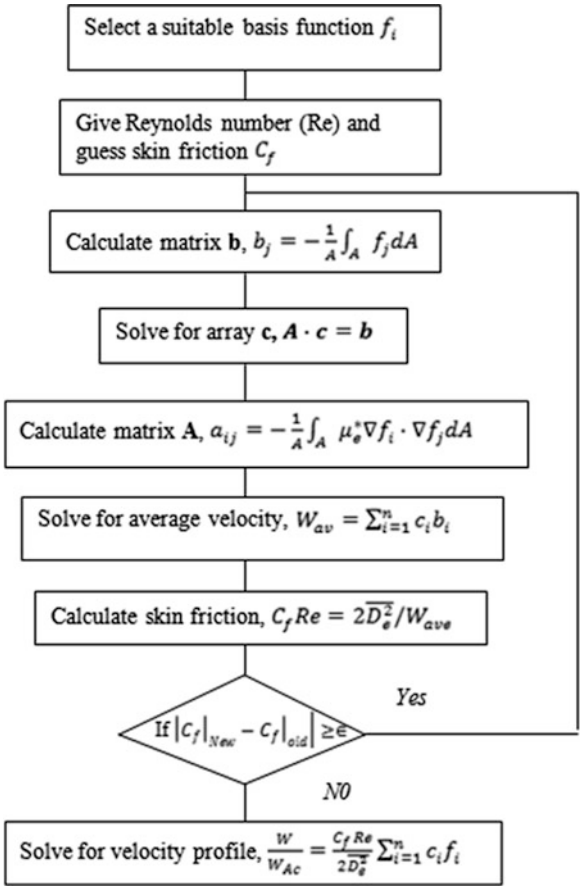

Fig. 10.2 Calculation procedure for turbulent flow

The Galerkin solution can be found by writing Eq. (9) for cylindrical coordinates as Galerkin's solution to this differential equation will be in the form of

$$\int_0^1 \phi_i(R)\left\{\frac{1}{R}\frac{d}{dR}\left(R\frac{d}{dR}\sum_{j=1}^{n} c_j\phi_j(R)\right)+1\right\}dR = 0$$

That can be written in form of a set of linear equations as

$$A_{ij} \cdot C_j = B_i$$

where

$$A_{ij} = \int_0^1 \phi_i(R)\left\{\frac{1}{R}\frac{d}{dR}\left(R\frac{d}{dR}\phi_j(R)\right)\right\}\mathrm{dR} \quad \text{and} \quad B_i = \int_0^1 \phi_i(R)dR$$

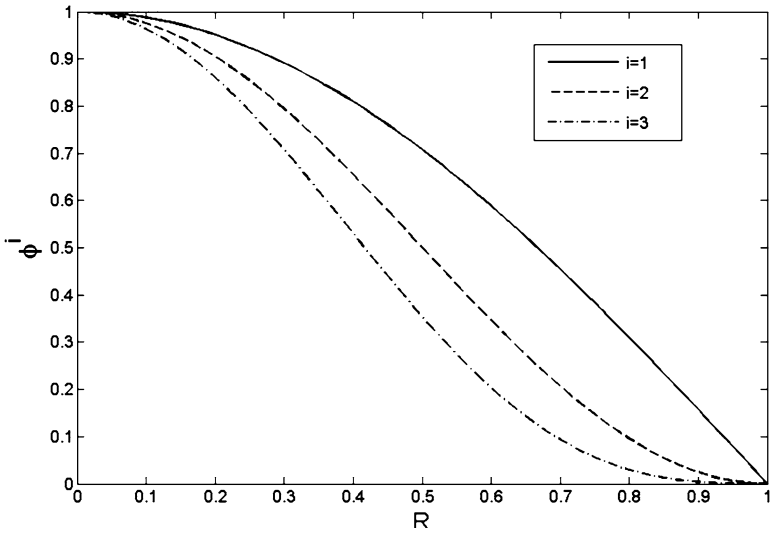

Fig. 10.3 Basis function for a flow in a cylindrical pipe

The Galerkin method starts with selecting the basis functions. The basis functions must satisfy the same boundary condition as governing equation. A suitable basis function can be in the form of $\phi_i(R)| = \left[\cos(\frac{\pi}{2}R)\right]^i$. Figure 10.3 illustrates the basis functions for n = 1,2,3.

A program in MATHLab was developed to evaluate matrics A_{ij}, B_i, C_j, and f for different value of n. Following is calculation for n = 4:

$$A_{ij} = \begin{bmatrix} -2.6882 & -3.3870 & -3.9424 & -4.4201 \\ -2.2171 & -3.2451 & -3.9434 & -4.4945 \\ -1.9310 & -3.0478 & -3.8335 & -4.4488 \\ -1.7334 & -2.8641 & -3.6957 & -4.3559 \end{bmatrix},$$

$$B_i = [-0.6366 \ -0.5000 \ -0.4244 \ -0.3750],$$

$$\text{and} \quad C_j = \begin{bmatrix} 0.3180 \\ -0.0974 \\ 0.0385 \\ -0.0091 \end{bmatrix}$$

The result for skin friction is given in the following table for different value of n:

n	**1**	**2**	**3**	**4**	**5**	**6**
$C_f \cdot R_e$	73.0132	63.7913	64.0286	63.9969	64.0004	63.9999

As the table indicates with only two terms the resistance coefficient can be evaluated with an error of 0.3%.

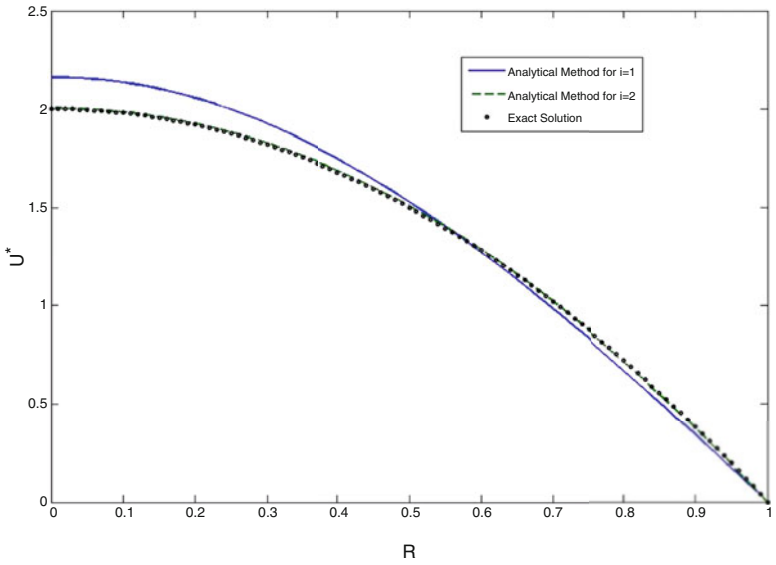

Fig. 10.4 Comparison of analytical and exact solution velocity profile

The velocity profile can be evaluated from

$$v = \sum_{i=1}^{n} C_i \cdot \phi_i$$

For example, for n = 4 velocity profile will be

$$v = 0.3180\cos(\pi/2R) - 0.0974\cos^2(\pi/2R) + 0.0385\cos^3(\pi/2R) - 0.0091\cos^4(\pi/2R)$$

As this figure indicates analytical and exact solutions are in excellent agreement with each other even with two-term solution ($n = 2$) for the velocity (Fig. 10.4). Another basis function that satisfies boundary condition and provides great accuracy is in the form of

$$f_i = (1 - R^2)R^{2(i-1)} \tag{16}$$

The first basis function in this set ($f_1 = 1 - R^2$) matches with the exact solution, and the method and one-term solution will match perfectly with exact solution.

Example 2: Laminar Flow Inside Square Duct

The governing equations in general for pipe flow are Navier–Stokes equations for incompressible laminar steady-state flow and can be written as

$$-\frac{dP}{dz}+\mu\left(\frac{\partial^2 u}{\partial x^2}+\frac{\partial^2 u}{\partial y^2}\right)=0$$

where u(x, y) is velocity in two dimensions with boundary condition of u(x, y) = 0 at the wall and dP/dz is pressure drop and μ is viscosity.

For a square channel with side "a," assuming $X=\frac{x}{a}$ and $Y=\frac{y}{a}$ the equation can be written in nondimensional form

$$1+\frac{\partial^2 U}{\partial X^2}+\frac{\partial^2 U}{\partial Y^2}=0 \tag{17}$$

where $U=-\frac{\mu/a^2}{dP/dz}u$ with the boundary condition of U = 0 for X = 0, Y = 0, X = 1, and Y = 1.

The following figure illustrates the geometry of such a channel:

Galerkin method starts with assuming a set of basis function then

$$U=\sum_{i=1}^{k} C_i\phi_i$$

where ϕ_i is the basis function that should satisfy the boundary condition (zero velocity on walls). One satisfactory expression for this function can be in the form of

$$\phi_i=\cos^m(\pi X)\cdot\cos^n(\pi Y)$$

where m and n are any set of integer numbers greater than zero. The following table can represent one set of such numbers that has been used in this study:

i	m	n
1	1	1
2	1	2
3	2	1
4	2	2
5	3	1
6	3	2
.	.	.
.	.	.

The following figures illustrate the shape of basis functions (ϕ_1 and ϕ_3) along X axis and Y = 0.3 (Fig. 10.5).

Multiplying both sides of Eq. (17) with the basis function and integrating over the domain, the governing equation will be changed to integral equation as

$$\int_{-1/2}^{1/2}\int_{-1/2}^{1/2}\phi_i(x)\left\{1+\left(\frac{\partial^2}{\partial X^2}+\frac{\partial^2}{\partial Y^2}\right)\left[\sum_{j=1}^{n} c_j\phi_j(x)\right]\right\}dx=0$$

And this integral equation can be converted to a set of linear equation as

$$A_{ij}\cdot C_j=B_i$$

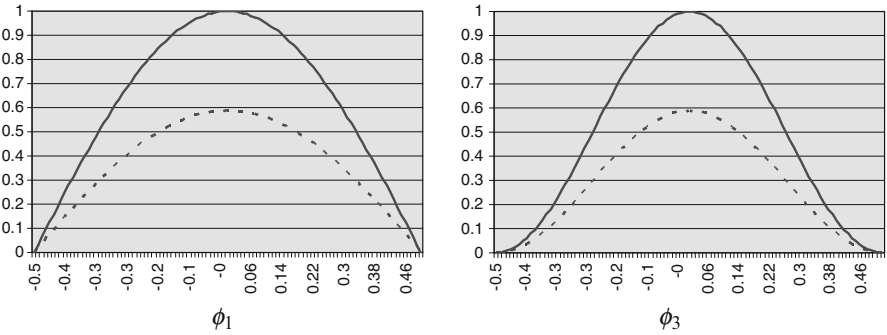

Fig. 10.5 Basis function for a flow in a square closed channel

where

$$A_{ij} = \int_{-1/2}^{1/2}\int_{-1/2}^{1/2} \phi_i(x)\left\{(\frac{\partial^2}{\partial X^2} + \frac{\partial^2}{\partial Y^2})\phi_j(x)\right\} dXdY$$

$$B_i = \int_{-1/2}^{1/2}\int_{-1/2}^{1/2} \phi_i(x) dXdY$$

To solve the problem B_i and A_{ij} must be evaluated. Following is a sample of calculation for $i = j = 1$ where $\phi_1 = \cos(\pi X)\cdot\cos(\pi Y)$:

$$B_1 = \int_{-1/2}^{1/2}\int_{-1/2}^{1/2} \phi_1 dXdY = \int_{-1/2}^{1/2}\int_{-1/2}^{1/2} \cos(\pi X)\cos(\pi Y) dXdY$$

$$= \frac{1}{\pi}\sin(\pi X)|_{-1/2}^{1/2} \cdot \frac{1}{\pi}\sin(\pi Y)|_{-1/2}^{1/2}$$

$$B_1 = \frac{4}{\pi^2}$$

For A_{11} second partial derivative of basis functions must be calculated first before integrating over the area:

$$\frac{\partial\phi_1}{\partial X} = -\pi\sin(\pi X)\cdot\cos(\pi Y) \quad \text{and} \quad \frac{\partial^2\phi_1}{\partial X^2} = -\pi^2\cos(\pi X)\cdot\cos(\pi Y)$$

$$\frac{\partial\phi_1}{\partial X} = -\pi\cos(\pi X)\cdot\sin(\pi X) \quad \text{and} \quad \frac{\partial^2\phi_1}{\partial X^2} = -\pi^2\cos(\pi X)\cdot\cos(\pi X)$$

and

$$\frac{\partial^2\phi_1}{\partial X^2} + \frac{\partial^2\phi_1}{\partial Y^2} = -2\pi^2\cos(\pi X)\cdot\cos(\pi X)$$

then

$$A_{ij} = \int_{-1/2}^{1/2}\int_{-1/2}^{1/2} \cos(\pi X)\cdot\cos(\pi Y)\cdot(-2\pi^2\cos(\pi X)\cdot\cos(\pi Y)) dXdY$$

$$A_{ij} = -2\pi^2 \int_{-1/2}^{1/2} \cos^2(\pi X) dX \int_{-1/2}^{1/2} \cos^2(\pi Y) dY$$

$$A_{ij} = -2\pi^2 \int_{-1/2}^{1/2} \frac{1}{2}(1-\cos(2\pi X)) dX \int_{-1/2}^{1/2} \frac{1}{2}(1-\cos(2\pi Y)) dY$$

$$A_{ij} = -\frac{\pi^2}{2}$$

Velocity coefficient will be calculated from $A_{11} \cdot C_1 = B_1$

$$C_1 = B_1/A_{11} = \frac{8}{\pi^4} = .08213$$

The result for six terms is as follows:

$$B = \begin{bmatrix} -0.4053 \\ -0.3183 \\ -0.3183 \\ -0.2500 \\ -0.2702 \\ -0.2122 \end{bmatrix} \quad A = \begin{bmatrix} -4.9348 & -4.1888 & -4.1888 & -3.5556 & -3.7011 & -3.1416 \\ -4.1888 & -4.3180 & -3.5556 & -3.6652 & -3.1416 & -3.2385 \\ -4.1888 & -3.5556 & -4.3180 & -3.6652 & -4.1888 & -3.5556 \\ -3.5556 & -3.6652 & -3.6652 & -3.7011 & -3.5556 & -3.5605 \\ -3.7011 & -3.1416 & -4.1888 & -3.5556 & -4.3180 & -3.6652 \\ -3.1416 & -3.2385 & -3.5556 & -3.5605 & -3.6652 & -3.6240 \end{bmatrix}$$

$$C = \begin{bmatrix} 0.188037 \\ -0.083799 \\ -0.131458 \\ 0.091192 \\ 0.045730 \\ -0.036434 \end{bmatrix}$$

Figure 10.6 illustrates the velocity profile in different locations from the center of the channel. The maximum velocity will be at location $X = 0$ and $Y = 0$ with a value of $U_{\max} = 0.0735$.

Figure 10.7 illustrates the same data in three-dimensional format.

The normalized velocity can be evaluated from Eq. (15) to be compared with other studies and experimental values. The normalized velocity at the center of the channel with this study is **s**

$$\frac{u_{\max}}{u_{ave}} = 2.093$$

This result was compared to an experimental study by Kakac et al. [5] and a finite difference method by the author. The experimental method is given for rectangular channels as

$$\frac{u}{u_{max}} = \left(\frac{m+1}{m}\right)\left(\frac{n+1}{n}\right)$$

$$m = 1.7 + 0.5\alpha^{*-1.4}$$

$$n = \begin{cases} 2 & for\ \alpha^* \le \frac{1}{3} \\ 2 + 0.3\left(\alpha^* - \frac{1}{3}\right) & for\ \alpha^* \ge \frac{1}{3} \end{cases}$$

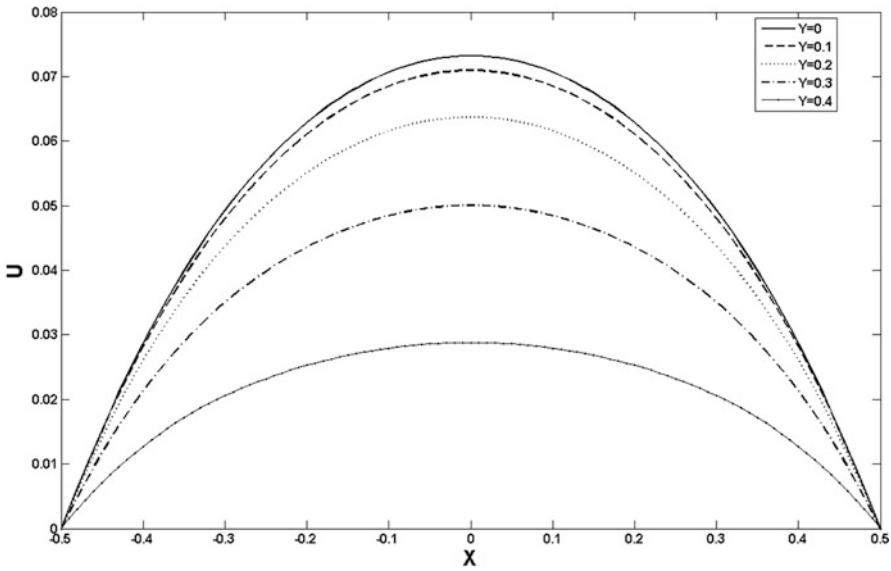

Fig. 10.6 Velocity profile inside a square channel

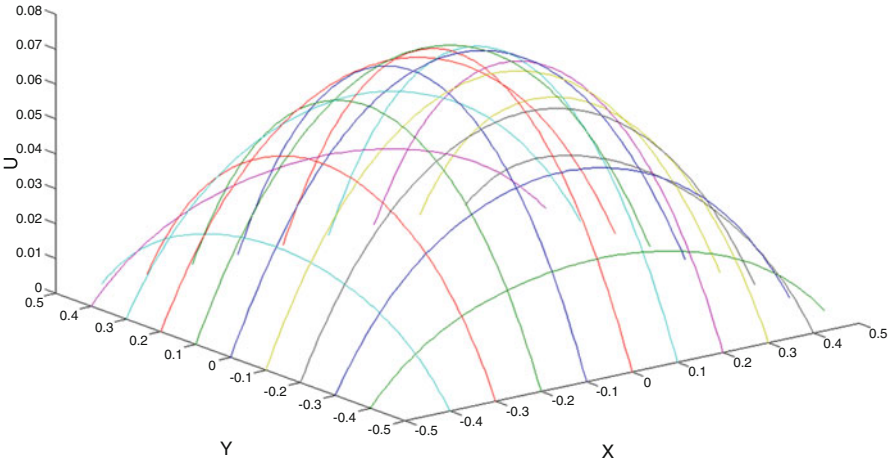

Fig. 10.7 Velocity profile inside a square channel

where $\alpha^* = 1$ for square channel; as a result $m = n = 2.2$ and the maximum velocity will be

$$\frac{u_{\max}}{u_{ave}} = 2.115$$

This is in good agreement with result evaluated by Galerkin-based solution.

The finite difference method yields this value as 2.099 using 101×101 elements. Finite difference method takes significant computational time for converging results.

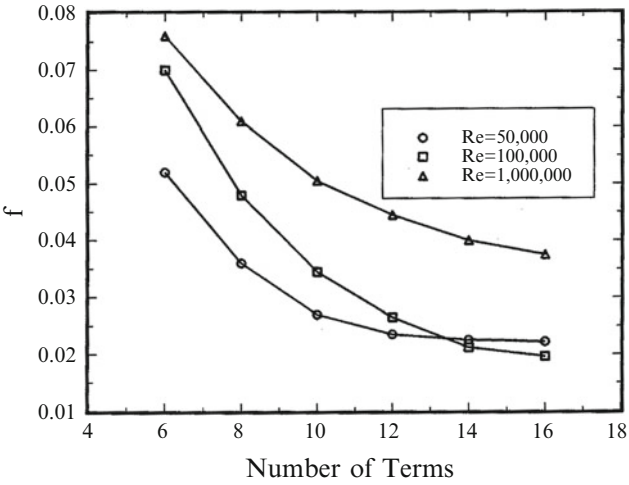

Fig. 10.8 Convergence of skin friction using polynomial basis function

Example 3: Turbulent Pipe Flow

The same procedure as example 1 is used for studying the turbulent flow in a circular pipe. The initial attempt is to use the same basis polynomial functions as introduced in example 1, Eq. (16). Although f_i in Eq. (16) is a simple function of R, the **a** matrix cannot be calculated analytically because of the existence of μ_e^* in Eq. (9) which is a function of r. Numerical integration is used to evaluate the members of the **a** matrix. The array **g**, however, is the same as that given for laminar flow.

Having matrix **a** and array **b** available, the skin friction and the velocity profile are calculated by an iterative procedure as shown in Fig. 10.8. The calculations show that the convergence of the results for skin friction requires a large number of the basis functions. This is the initial difficulty encountered when calculating pressure drop in turbulent flow by the standard GBI method. In contrast, the laminar flow requires as few as two basis functions for an accurate solution.

Figure 10.8 shows the convergence of the results for Reynolds numbers $5 \times 10^4, 10^5$, and 10^6 using a different number of terms. This figure confirms that a higher Reynolds number requires more terms to have convergence. It is also noticed that the upper limit for N is 16. For values of N greater than 16, the matrix inversion routine fails, and convergence never happens. According to Fig. 10.8, solutions for a Reynolds number of 10^6 or higher cannot be obtained.

The velocity profile for Reynolds number 10^5 and for different values of N is given in Fig. 10.9. The computed results are compared with the experimental data given by Nikuradse [9] for the same Reynolds number. This figure shows that, as the number of terms increases, the calculated velocity profile gets closer to the experimental data. For N=16, which satisfies the convergence, the calculated velocity is in agreement with the experimental data within 3%.

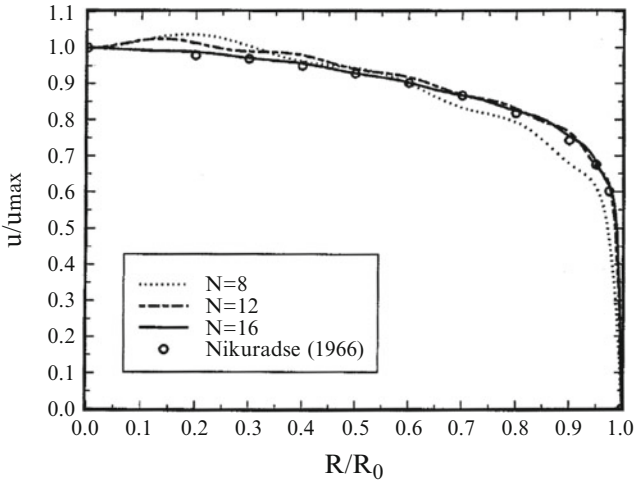

Fig. 10.9 Predicted velocity profile by using polynomial basis functions

The calculated values of skin friction and velocity profile, Figs. 10.8 and 10.9, require a large number of terms to achieve convergence. Increasing the number of terms increases the computer time and reduces the accuracy of the results. For these reasons, selecting a set of basis functions that describes the behavior of the turbulent velocity profile is necessary. The following basis functions have the necessary characteristics to describe the turbulent velocity profile:

$$f_i = \{1 - e^{[-\beta(1-R^2)]}\}R^{2(i-1)} \tag{18}$$

The factor $1 - e^{[-\beta(1-R^2)}$ in Eq. (18) is a turbulence factor that depends on the Reynolds number. It provides a sharp slope for the velocity profile at the wall and disappears far from the wall. The factor B is a constant that depends on the turbulence similar to A in the turbulent viscosity equation of Van Driest. The value of β is arbitrarily selected equal to one for laminar flow.

The computed results for three different Reynolds numbers are given in Fig. 10.10. This figure illustrates that the calculated skin friction decreases by increasing the coefficient β, then begins to increase as β increases. A value of β that makes the skin friction minimum is the proper choice. A justification of selecting β at minimum skin friction is given in the Appendix. The calculated skin friction at the optimum β provides the best agreement with the experimental values.

The optimum values of β, for different Reynolds numbers, were calculated, and method of least square was used to find correlation for β and skin friction as given in the following equation:

$$B = \frac{C_f Re}{19}$$

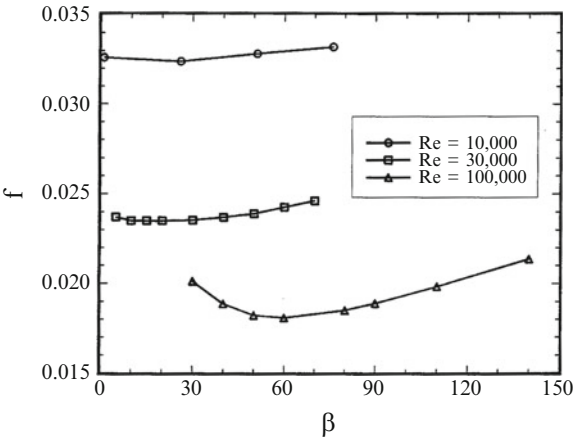

Fig. 10.10 Calculated skin friction for different values of β

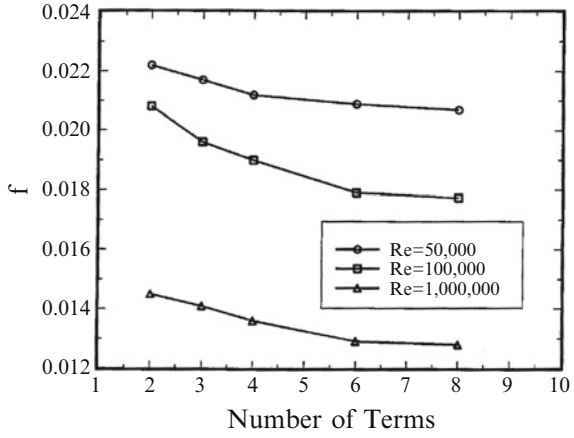

Fig. 10.11 Convergence of the result by using new basis functions

Once a correlation for β is available, one can proceed to solve for velocity profile and skin friction at any Reynolds number. Figure 10.11 shows the convergence of skin friction for three different Reynolds numbers versus the number of terms, N. A comparison between the data in Figs. 10.8 and 10.11shows that the new basis functions provide convergence with fewer terms. In fact, for a small Reynolds number $(\mathrm{Re} = 50,000)$, two terms in the series give the skin friction that has a satisfactory agreement with the experimental values.

The analysis also shows a good agreement with the experimental velocity profile given by Laufer [7]. The experimental data of Laufer [7] are given in Fig. 10.12 and compared with the analytical results for this study when $\mathrm{N} = 2, 4$, and 8. The figure shows the agreement between analytical and experimental velocity profiles to within 6% using as few as 2 terms in the series.

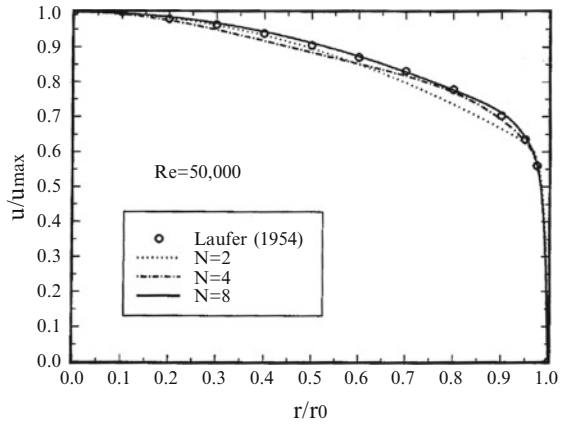

Fig. 10.12 Velocity profiles for 2, 4, and 8 terms in series

The velocity profiles, using 8 terms, and the experimental data of Laufer[7] for $\mathrm{Re} = 5 \times 10^4$ and 5×10^5 and Nikuradse [9] are shown in Fig. 10.13. Both calculated velocity profiles agree with the experimental measurements to within 3%. For more than 8 terms, no significant improvement is observed.

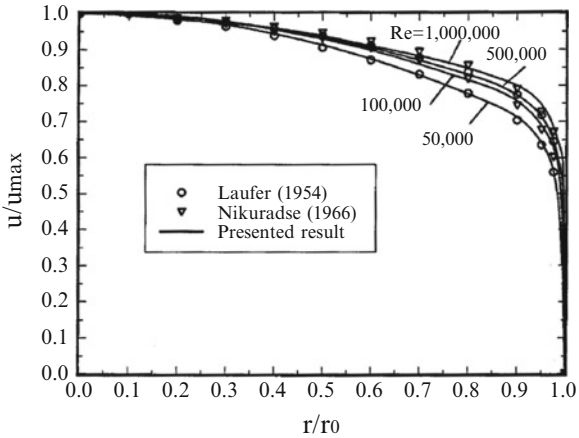

Fig. 10.13 Comparison of predicted velocity profile and experimental data

Conclusions

A simple Galerkin-based solution has been presented that predicts the skin friction and velocity flow field in fully developed duct flow. The analytical steps, described in this study, apply to both laminar and turbulent flow in ducts with various cross-

sectional shapes. A comparison of the calculated values with the experimental data shows satisfactory agreement leading to the following major conclusions.

The solution for turbulent flow shows that special care must be taken in selecting basis functions. A suitable set of basis functions reduces the number of terms in the series, N, and consequently decreases computing time and increases the accuracy of the results. The value of $N = 8$ provides data with good accuracy over a rather large range of the Reynolds number, $4 \times 10^4 < Re < 10^6$. Even for $Re < 10^5$ the method provides an accurate solution with as few as two terms.

It is shown that the modified Van Driest model for effective viscosity given by Richman and Azad [10] is a sufficiently accurate model for predicting turbulence. The calculated Nusselt numbers based on this model show good agreement with the correlation of Gnielinski [2].

Appendix

Highlights of the Variational Steps

The details of the minimization principle are provided by Ghariban [3]; only a brief description is given here. The Galerkin method is based on minimization of the integral

$$I = \int_A \left\{ \frac{1}{2}\mu_e^*(X,Y) \left[\left(\frac{\partial W}{\partial X} \right)^2 + \left(\frac{\partial W}{\partial Y} \right)^2 \right] + W \right\} dA \tag{19}$$

In the minimization of Eq. (19), it is assumed that μ_e^* is a known function of X and Y. The variational steps begin by replacing W by $\overline{W}$ and then setting $\overline{W}(X,Y) = W(X,Y) + \varepsilon\eta(X,Y)$. The calculation of $(\partial I/\partial\varepsilon)$ as $\varepsilon \to 0$ leads to the equation [6],

$$\int_A \eta(X,Y) \lfloor 1 - \nabla_1 \cdot (\mu_e^* \nabla_1 W) \rfloor dA = 0 \tag{20}$$

where $\eta(X,Y)$ is an arbitrarily selected function. The Galerkin method uses Eq. (20) to compute $W(X,Y)$. For example, one substitutes for $W(X,Y)$ in Eq. (20) a quantity

$$W(X,Y) = \sum_{i=1}^{N} d_i f_i(X,Y) \tag{21}$$

and replaces the arbitrary function $\eta(X,Y)$ by $f_J(X,Y)$ for $j = 1,2,\ldots,N$. It is to be noted that μ_e is assumed to be a known function of X and Y. This yields the Galerkin solution described by Eq. (8). For turbulent flow, $\mu_e^*(X,Y)$ is a function of shear stress at the wall, and shear stress is unknown. One must provide a value for the shear stress and then solve for velocity field. The subsequent calculation of shear stress from computed velocity field should be followed by recalculation of the velocity field. The continuation of this iterative procedure leads to a Galerkin-type solution.

For turbulent flow, the numerical studies show that the number of terms using $f_i(X,Y)$ functions with simple forms, Eq. (20), can be prohibitively large. It is suggested, in this paper, to introduce a new form for $f_i(X,Y)$, Eq. (21), that changes as the shear stress changes. The iterative minimization procedure, using this latter form of $f_i(X,Y,B)$ with an additional parameter B, needs some modifications. The first step of iteration is to consider a known value for B and solve for $W(X,Y)$ using the standard Galerkin solution method. A selected value of B influences the value of the calculated average shear stress, and B represents the effect of the turbulence intensity on the velocity profile. The minimization of function I, following some algebra [3], leads to an additional equation

$$\int_A \frac{\partial \mu_e^*(X,Y)}{\partial B} dA \left[\left(\frac{\partial W}{\partial X} \right)^2 + \left(\frac{\partial W}{\partial \mathrm{Y}} \right)^2 \right] dA = 0 \tag{22}$$

Because $(\partial W/\partial X)^2 + (\partial W/\partial Y)^2 > 0$, the integral given by Eq. (22) is zero if $(\partial \mu_e^*/\partial B) = 0$. For turbulent flow, it is assumed that B in Eq. (21) depends on the average shear stress, τ_w . Therefore, the minimization of I requires that $(\partial \mu_e^*/\partial \tau_w)(\partial \tau_w/\partial B) = 0$ in addition to Eq. (20). For turbulent flow, the effective viscosity coefficient, μ_e^*, increases as τ_w increases, indicating $\partial \mu_e^*/\partial \tau_w > 0$; then I is minimum if $\partial \tau_w/\partial B = 0$. The dimensionless form of this condition is used in subsequent calculations; that is, B is computed so that

$$\frac{\partial C_f}{\partial B} = 0$$

Acknowledgment I thank all reviewers and contributors for their valuable suggestions, comments, and correction in the final version of my manuscript. They were able to constructively pinpoint relevant issues that need to be revised in my manuscript and which will strengthen and improve my paper.

References

1. Beck, J.V., Cole, K.D., Haji-Sheikh, A., Litkouhi, B.: Heat Conduction Using Green's Functions, Chapter 11. Hemisphere Publishing, Washington, D.C. (1992)
2. Gnielinski, V.: New equations for heat and mass transfer in turbulent pipe and channel flow. Int. Chem. Eng. **16**, 359–468 (1976)
3. Ghariban, N.: Turbulent flow and heat transfer in ducts. PhD. Thesis, Department of Mechanical Engineering, The University of Texas at Arlington (1993)
4. Haji-Sheikh, A., Mashena, M., Haji-Sheikh, M.J.: Heat transfer coefficient in ducts with constant wall temperature. J. Heat Tran. **105**, 878–883 (1983)
5. Kakac, S., Shah, R., Aung, W.: Handbook of Single-Phase Convective Heat Transfer, Chapter 2. Wiley, New York (1987)
6. Kantorovitch, L.V., Krylov, V.I.: Approximate Methods of Higher Analysis. Wiley, New York (1960)
7. Laufer, J.: The structure of turbulence in fully developed pipe flow. NACA Rept. 1174 (1954)

8. Malhotra, A., Kang, S.S.: Turbulent prandtl number in circular pipes. Int. J. Heat Mass Tran. **27**(8), 2158–2161 (1984)
9. Nikuradse, J.: Gesetzmabigkiten der turbulenten stromung in glatten Rohen. Forsch. Arb. Ing.-Wes. **356** (1932); English transl., NASA TT F-10, 359 (1966)
10. Richman, J.W., Azad, R.S.: Developing turbulent flow in smooth pipes. Appl. Sci. Res. **28**, 419–440 (1973)
11. Van Driest, E.R.: On turbulent flow near a wall. J. Aeronaut. Sci. **23**, 1007–1012 (1956)

Nomenclature

A	Characteristic length
a_{ij},b_{ij},c_{ij}	Element of matrices **A**,**B**,**C**
A	Flow area of duct
A^+	Damping constant
A,**B**,**C**	Matrices
β	Constant in Eq. (12)
c_i	Element of the array **c**
c	Array of velocity coefficient
C_f	Friction factor
C_n	Temperature profile coefficient
D_e	Hydraulic diameter
$\overline{D_e}$	Hydraulic diameter, dimensionless
f_i	Basis function
g_i	Element of the array **g**
g	Auxiliary array
i, j	Indices
N	Number of terms in series
P	Static pressure
r	Cylindrical coordinate, dimensionless
R	Cylindrical coordinate
R_o	Pipe radius
T	Local temperature
T'	Fluctuating temperature
u', v', w'	Fluctuating velocity components
u^+	Velocity parameter
w	Axial velocity
W	Axial velocity, dimensionless
w_{av}	Average velocity
W_{av}	Average velocity, dimensionless
X, Y, Z	Coordinates
X, Y, Z	Coordinates, dimensionless
y^+	Wall distance parameter

κ	Von Karman constant
μ	Molecular viscosity
μ_e	Effective viscosity
μ_e^*	Effective viscosity, dimensionless
μ_t	Turbulent viscosity
μ_t^*	Turbulent viscosity, dimensionless
ρ	Fluid density
τ_w	Wall shear stress